Hemispheric Helicity Trend for Solar Cycle 23

Alexei A. Pevtsov
National Solar Observatory/Sacramento Peak[1], *PO Box 62, Sunspot, NM 88349, U.S.A.*
apevtsov@sunspot.noao.edu

Richard C. Canfield
Department of Physics, Montana State University, Bozeman, MT 59717-3840, U.S.A.
and

Sergei M. Latushko
Institute of Solar-Terrestrial Physics, Russian Academy of Sciences, PO Box 4026, Irkutsk 664033, RUSSIA

ABSTRACT

Applying the same methods we used in solar cycle 22, we study active region vector magnetograms, full disk X-ray images, and full disk line-of-sight magnetograms to derive the helicity of solar magnetic fields in the first four years of solar cycle 23. We find that these three datasets all exhibit the same two key tendencies – significant scatter and weak hemispheric asymmetry – as were observed in solar cycle 22. This supports the interpretation of these tendencies as signatures of the writhing of magnetic flux by turbulence in the convection zone.

Subject headings: Sun: magnetic fields—Sun: corona—Sun: activity

1. Introduction

Solar cycle 22 ended in 1996, and the new solar cycle became dominant in early 1997 (de Toma et al. 2000). During cycle 22 the hemispheric helicity trend was the subject of many studies, reviewed by Brown, Canfield & Pevtsov (1999), which used photospheric vector magnetograms, coronal X-ray images, and full-disk line-of-sight photospheric magnetograms.

Pevtsov et al. (1995) and Longcope et al. (1998) used photospheric active-region vector magnetograms from the Haleakala Stokes Polarimeter (HSP: Mickey 1985) at Mees Solar Observatory to compute values of the linear force-free field α coefficient. They found $\alpha < 0$ for 69% and 66% respectively of regions in the northern hemisphere and $\alpha > 0$ for $\sim$ 75% and 62% respectively of those in the southern hemisphere. On the other hand, Abramenko et al. (1997) and later Bao & Zhang (1998) used vector magnetograms from the Huairou Solar Observing Station to compute the fractional imbalance of current helicity density (h_c) and found a stronger hemispheric asymmetry. These authors found $h_c < 0$ for 84% and 84% of regions respectively in the northern hemisphere, and $h_c > 0$ for 86% and 79% respectively in the southern hemisphere. Bao et al. (2000) attributed this difference to the different helicity measures used (α vs h_c), although Faraday rotation may also affect the measurements (Hagyard & Pevtsov 1999; Bao et al. 2000; Zhang 2001).

These works all show that the hemispheric helicity sign asymmetry is just a tendency, not a rigid rule. This is an important point, since some individual mechanisms of helicity generation, such

[1]Operated by the Association of Universities for Research in Astronomy, Inc (AURA), for the National Science Foundation.

as differential rotation (DeVore 2000), generate a rigid hemispheric rule, not a weak tendency. Although some dynamo models can give mixed helicity (Gilman & Charbonneau 1999), their predicted current helicity density falls short of observed amplitudes by an order of magnitude (Longcope et al. 1999). For these reasons, it is noteworthy that the writhing of magnetic flux by turbulence in the convection zone (the Σ effect, Longcope et al. 1998) has recently been shown to be consistent with both the sign of the hemispheric tendency and the amplitude of its scatter.

Rust & Kumar (1996) and Canfield & Pevtsov (1999) used X-ray images from the Yohkoh Soft X-ray Telescope (SXT: Tsuneta et al. 1991) to study the hemispheric dependence of the the shapes of sigmoidal coronal loops. They found that 69% (59% in Canfield & Pevtsov) of such loops in the northern hemisphere had inverse-S shape, and 69% (68%) in the southern hemisphere had S-shape. This hemispheric asymmetry is consistent with the photospheric helicity distribution.

Pevtsov & Latushko (2000) reconstructed the large-scale solar vector magnetic field using full disk longitudinal magnetograms from the SOHO Michelson Doppler Imager (MDI: Scherrer et al. 1995). They computed latitudinal profiles of the current helicity density for 7 solar rotations (June–November 1996) near the end of cycle 22. They found the hemispheric trend in sign of the current helicity density on large scales to be in agreement with that of photospheric active regions and the corona.

To understand the origin of the hemispheric helicity trend it is important to determine how it varies with the solar cycle. For example, if the Coriolis force is important, we do not expect solar-cycle dependence. A modern interpretation of early Hα observations of vortex patterns around sunspots (Hale 1927; Richardson 1941) supports this expectation. The notion that the hemispheric helicity trend is not solar cycle dependent has already been expressed in several recent works (e.g., Bothmer & Rust 1997; Bao & Zhang 1998; Pevtsov & Canfield 1999, 2000). However, the data used for these claims have been limited to just a few regions of the new cycle. Moreover, Bao, Ai & Zhang (2000) have found recently that in their data, the hemispheric asymmetry at the beginning of cycle 23 is opposite in sign to that found in cycle 22. However, this may be an artifact that accrues from the Faraday effect in their line-center transverse-field measurements.

In the present Letter we study the hemispheric helicity trend in the solar cycle 23 using the data same sources – HSP photospheric vector magnetograms, SXT full-disk X-ray images, and SOHO/MDI full-disk longitudinal magnetograms – and methods as we used in the cited studies during cycle 22. We find that the hemispheric helicity trend during the first four years of cycle 23 is the same as that for cycle 22, by all three measures.

2. Observations

We study HSP vector magnetograms of 263 active regions observed between July, 1997 and September, 2000. We compute the α_{best} coefficient $(\nabla \times \mathbf{B}) = \alpha_{best}\mathbf{B}$, (Pevtsov et al. 1995) and the fractional imbalance of the current helicity density h_c (the ratio of net and total unsigned helicity density, e.g., Abramenko et al. 1997). We follow the same procedure as Pevtsov et al. (1995) for azimuth ambiguity resolution and α_{best} determination. Figure 1 compares the latitudinal variation of α_{best} for the first four years of solar cycle 23 (lower panel) to that of the maximum and declining phase of solar cycle 22 (upper panel), from Longcope et al. (1998). The same basic features – large scatter and weak, but noticeable, hemispheric preference – are present in both. The tendency for active regions to appear at lower latitudes during the declining phase than the rising phase is evident, but unimportant for our purposes, when the two panels of Figure 1 are compared. In the cycle 23 data set, 62.9% of 140 active regions in the northern hemisphere have $\alpha_{best} < 0$ and 69.9% of 123 regions in the southern hemisphere have $\alpha_{best} > 0$, consistent with cycle 22. The current helicity imbalance (h_c) shows a weaker hemispheric tendency than α_{best}: 50% of 140 active regions in the northern hemisphere have $h_c < 0$ and 57.5% of 120 regions in the southern hemisphere have $h_c > 0$.

To study the helicity of coronal structures we follow the same procedure as Canfield & Pevtsov (1999). We employ SXT full disk movies in videodisk form for January 1997 – August 2000. We identify sigmoidal structures, their shape and their hemisphere. Table 1 shows a clear hemispheric preference in the distribution of loops by shape. The hemispheric trend in coronal magnetic fields during first four years of solar cycle 23 is a statistical preference for S-shaped sigmoids in the south and inverse-S in the north, in agreement with solar cycle 22 (Rust & Kumar 1996; Canfield & Pevtsov 1999 (tabulated); Pevtsov & Canfield 2000).

We study the large-scale photospheric helicity using full disk SOHO/MDI magnetograms from December 1996 – November 1997, early in solar cycle 23, applying the same procedure used late in cycle 22 by Pevtsov & Latushko (2000). Because the strong and evolving magnetic fields of active regions contribute to increased scatter in averaged large-scale helicity profile when this method is used (cf. error bars in middle and low latitudes on Figure 2), we restrict this study to these periods of relatively low solar activity early in cycle 23. Figure 2 compares the averaged latitudinal profile of h_c for these two periods in cycle 22 (upper panel) and cycle 23 (lower panel). Within what we believe to be the uncertainties, the results are the same for two cycles. There is no hemispheric preference in sign of large-scale helicity at low latitudes, but at high latitudes h_c is negative in the northern hemisphere, and positive in the southern, at the one sigma level. The lack of hemispheric asymmetry at low latitudes may be attributed to the influence of evolving strong magnetic fields of active regions, which invalidate the assumption of longitudinal symmetry used to compute the latitudinal profile (Pevtsov & Latushko 2000).

3. Discussion

The data presented in this Letter show that the hemispheric helicity asymmetry observed in solar cycle 22 does not reverse sign in cycle 23. In both cycles the α_{best} coefficient shows significant scatter and weak, but noticeable hemispheric asymmetry. This scatter and asymmetry is consistent with a modern interpretation of the early sunspot vortex results of Hale (1927) and Richardson (1941), originally attributed to hydrodynamic processes.

The physical origin of these properties is still being debated, but turbulent buffeting of magnetic flux tubes in the convection zone (the so called Σ-effect, Longcope et al. 1998) describes quite well both the weak hemispheric dependency of α_{best} and the significant scatter. The facts that the hemispheric dependency did not reverse its sign from cycle 22 to cycle 23, and that it has very similar trend and scatter in both cycles, support the Σ-effect interpretation. Alternative mechanisms, e.g., simple writhing of Ω-loops by the Coriolis force, overshoot region dynamos and differential rotation fail to explain some or all observed properties (Longcope et al. 1999; Pevtsov & Canfield 2000). However, recent studies (e.g., DeVore 2000; vanBallegooijen 1999) show that some of these processes may be important at some level.

The authors are pleased to acknowledge support by NASA through SR&T grant NAG5-6110 and the SXT contract NAS8-00119 at NASA Marshall Space Flight Center. We wish to thank the staff of the Mees Solar Observatory for the HSP data set, and a helpful referee for improving the manuscript. Yohkoh is a mission of ISAS in Japan. The SXT instrument is a collaboration of the University of Tokyo, the National Astronomical Observatory of Japan, and the Lockheed Martin Solar and Astrophysics Laboratory.

REFERENCES

Abramenko, V. I., Wang, T., & Yurchishin, V. B. 1997, Sol. Phys., 174, 291

Bao, S. & Zhang, H. 1998, ApJ, 496, L43

Bao, S.D., Pevtsov, A.A., Wang, T.J., & Zhang, H., 2000, Sol. Phys., 195, 75

Bao, S., Ai, G. X., & Zhang, H. Q. 2000, J. Astrophys. Astr, 21, 303

Bothmer, V. & Rust, D. M. 1997, in Coronal Mass Ejections, ed. N. Crooker, J. A. Joselyn, & J. Feynman (Washington, DC: AGU), 139

Brown, M., Canfield, R., & Pevtsov, A. 1999, Magnetic Helicity in Space and Laboratory Plasmas (Washington, DC: AGU)

Canfield, R. C. & Pevtsov, A. A. 1999, in Magnetic Helicity in Space and Laboratory Plasmas, ed. M. R. Brown, R. C. Canfield, & A. A. Pevtsov (Washington, DC: AGU), 197

de Toma, G., White, O. R., Harvey, K. L. 2000, ApJ, 539, 944

DeVore, C. R. 2000, ApJ, 539, 944

Gilman, P. A. & Charbonneau, P. 1999, in Magnetic Helicity in Space and Laboratory Plasmas, ed. M. R. Brown, R. C. Canfield, & A. A. Pevtsov (Washington, DC: AGU), 75

Hagyard, M. J. & Pevtsov, A. A. 1999, Sol. Phys., 189, 25

Hale, G. E. 1927, Nature, 119, 708

Longcope, D. W., Fisher, G. H., & Pevtsov, A. A. 1998, ApJ, 507, 417

Longcope, D., Linton, M., Pevtsov, A., Fisher, G., and Klapper, I. 1999, in Magnetic Helicity in Space and Laboratory Plasmas, ed. M. R. Brown, R. C. Canfield, & A. A. Pevtsov (Washington, DC: AGU), 93

Mickey, D. L. 1985, Sol. Phys., 97, 223

Pevtsov, A. A. & Canfield, R. C. 1999, in Magnetic Helicity in Space and Laboratory Plasmas, ed. M. R. Brown, R. C. Canfield, & A. A. Pevtsov (Washington, DC: AGU), 103

Pevtsov, A. A. & Canfield, R. C. 2000, J. Astrophys. Astr, 21, in press

Pevtsov, A. A., Canfield, R. C., & Metcalf, T. R. 1995, ApJ, 440, L109

Pevtsov, A. A. & Latushko, S. M. 2000, ApJ, 528, 999

Richardson, R. S. 1941, ApJ, 93, 24

Rust, D. M. & Kumar, A. 1996, ApJ, 464, L199

Scherrer, P. H. et al. 1995, Sol. Phys., 162, 129

Tsuneta, S. et al. 1991, Sol. Phys., 136, 37

van Ballegooijen, A. A. 1999, in Magnetic Helicity in Space and Laboratory Plasmas, ed. M. R. Brown, R. C. Canfield, & A. A. Pevtsov (Washington, DC: AGU), 213

Zhang, H., 2001, Sol. Phys., in press

This 2-column preprint was prepared with the AAS LaTeX macros v5.0.

Table 1: Hemispheric distributions of sigmoids

Cycle 22 (182 regions)	Forward-S	Inverse-S
Northern hemisphere	41%	59%
Southern hemisphere	68%	32%
Cycle 23 (90 regions)	Forward-S	Inverse-S
Northern hemisphere	25%	75%
Southern hemisphere	78%	22%

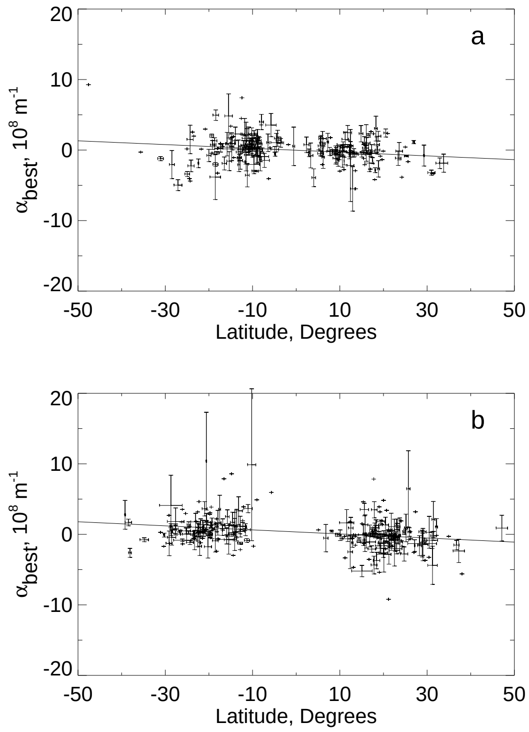

Fig. 1.— Latitudinal profile of α_{best} for (a) 203 active regions in cycle 22 (Longcope et al. 1998) and (b) 263 active regions in cycle 23 (this work). Error bars (when present) correspond to one standard deviation of the mean α_{best} from multiple magnetograms of the same active region. Points without error bars correspond to active regions represented by a single magnetogram. The solid line shows a least-squares best-fit linear function.

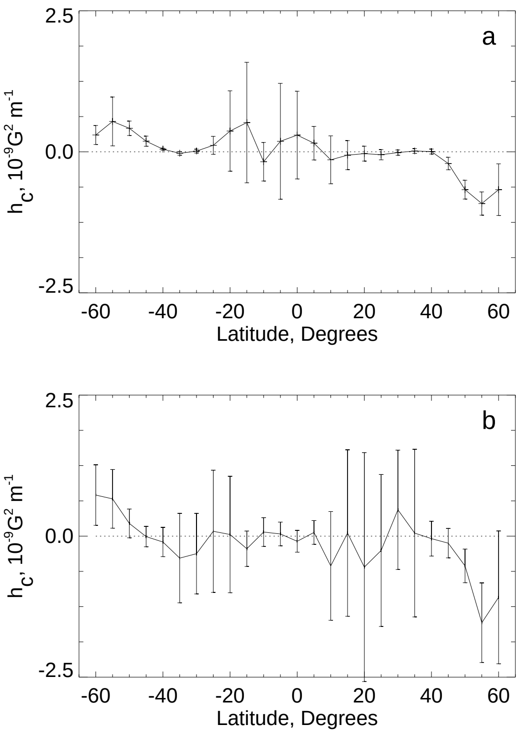

Fig. 2.— Latitudinal profile of h_c of the large-scale magnetic field (a) late in cycle 22 (Pevtsov & Latushko 2000) and (b) early in cycle 23 (this work). The error bars correspond to one standard deviation of the averaged h_c for 7 and 13 solar rotations in (a) and (b), respectively.